ISSN 1019-0643

PSI-Bericht Nr. 118
JEF REPORT 14
Februar 1992

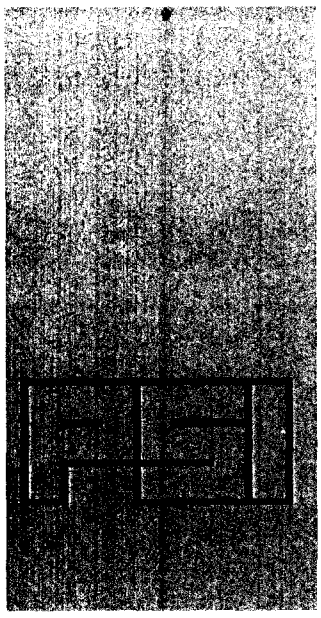

PSI-Bericht Nr. 118
JEF REPORT ~~14~~ 12

Paul Scherrer Institut

Labor für Reaktorphysik und Systemtechnik

Comparison Calculation of a Large Sodium-Cooled Fast Breeder Reactor Using the Cell Code MICROX-2 in Connection with ENDF/B-VI and JEF-1.1 Neutron Data

Sandro Pelloni

A report on work done in the frame of JEF activity under the leadership of OECD NEA DATA BANK (BANQUE DE DONNEES DE L'AEN OCDE)

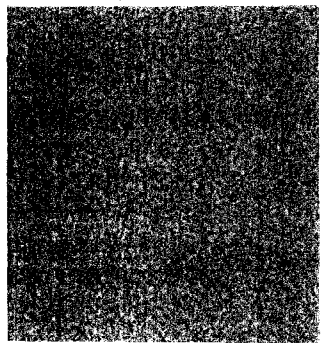

Paul Scherrer Institut
Würenlingen und Villigen
CH-5232 Villigen PSI

Telefon 056/99 21 11
Telex 82 74 14 psi ch
Telefax 056/98 23 27 PSI CH

PSI-Bericht Nr. 118

Comparison Calculation of a Large Sodium-Cooled Fast Breeder Reactor Using the Cell Code MICROX-2 in Connection with ENDF/B-VI and JEF-1.1 Neutron Data

by

S. Pelloni

Paul Scherrer Institute
Würenlingen and Villigen
CH-5232 Villigen PSI

February 1992

Abstract

We have obtained results for a large sodium-cooled fast breeder reactor benchmark using data from the ENDF/B-VI and from Revision 1 of the JEF-1 (JEF-1.1) evaluation. The required cross sections were processed with the NJOY code system (Version 89.62) and homogenized with the spectrum cell code MICROX-2. Multigroup transport-theory calculations in 33 neutron groups (forward and adjoint) were performed using the two-dimensional code TWODANT and kinetic parameters were determined using the first-order perturbation-theory code PERT-V. We calculated eigenvalues, neutron balance data, global and regional breeding and conversion ratios, central reaction rate ratios and reactivity worths with and without sodium, effective delayed neutron fraction and inhour reactivity, regional sodium void reactivity, and isothermal core fuel Doppler-reactivities. In particular, it is shown that good agreement (generally within one standard deviation) is achieved between these results and the average values over sixteen benchmark solutions obtained in the past. The eigenvalues predicted with ENDF/B-VI are up to 0.7% larger than those calculated with JEF-1.1 cross sections. This discrepancy is mainly due to different inelastic scattering cross sections for ^{23}Na and ^{238}U, and to different fast fission and nubar data for ^{239}Pu.

Zusammenfassung

Wir haben Vergleichsrechnungen zur Neutronik eines grossen natriumgekühlten schnellen Brutreaktors mit Hilfe nuklearer Daten aus der ENDF/B-VI- und aus einer revidierten Version der JEF-1-Grunddatenbibliothek (JEF-1.1) durchgeführt. Die benötigten Wirkungsquerschnitte wurden zunächst mit dem Programmsystem NJOY (Version 89.62) generiert und dann mit Hilfe des Spektralprogramms MICROX-2 homogenisiert. Anschliessend wurden direkte und adjungierte Flussrechnungen in 33 Neutronen-Gruppen mit dem zweidimensionalen Transportprogramm TWODANT durchgeführt und kinetische Parameter mit Hilfe der Störungstheorie erster Ordnung mit dem Programm PERT-V bestimmt. Es wurden Eigenwerte, Neutronen-Bilanz-Parameter, globale und zonenabhängige Brut- und Konversions-Raten, Verhältnisse von wichtigen Reaktionsraten im Zentrum des Reaktors, Reaktivitätskoeffizienten für Konfigurationen mit und ohne Natrium, der Anteil verzögerter Neutronen, die Generationszeit der prompten Neutronen, zonenabhängige Natrium-Voidkoeffizienten und isothermische Doppler-Reaktivitäts-Koeffizienten für den Brennstoff bestimmt. Es wird insbesondere gezeigt, dass diese neuen Resultate mit den Mittelwerten aus den sechzehn ursprünglich eingereichten Benchmark-Lösungen gut, d.h. meistens innerhalb einer Standard-Abweichung, übereinstimmen. Die Eigenwerte aus den Rechnungen mit ENDF/B-VI-Bibliotheken sind bis 0.7 % grösser als diejenigen, die man mit JEF-1.1-Wirkungsquerschnitten erhält. Diese Diskrepanz ist primär durch die verschiedenen inelastischen Streu-Querschnitte von ^{23}Na und ^{238}U und die abweichenden Daten für die schnelle Spaltung von ^{239}Pu bedingt.

Contents

1 INTRODUCTION 6

2 NUCLEAR DATA 7
- 2.1 NJOY Libraries . . . 7
- 2.2 MICROX-2 Libraries . . . 8
- 2.3 Delayed Neutron Libraries . . . 10

3 CODES 10
- 3.1 MICROX-2 . . . 11
- 3.2 ONEDANT and TWODANT . . . 12
- 3.3 PERT-V . . . 12

4 COMPUTATIONAL MODEL 13

5 RESULTS AND DISCUSSION 16

6 CONCLUSIONS AND RECOMMENDATIONS 18

List of Tables

1 Sigma-Zero Values by Isotope in the GENDF Data Files . . . 9

2 Eigenvalues k_{eff} for the Eight Configurations, Eigenvalue k_{∞} for the Inner Core (Configuration 1), Calculated Using JEF-1.1 Data, and Their Deviations from the Mean Benchmark Values . . . 20

3 Eigenvalues k_{eff} for the Eight Configurations, Eigenvalue k_{∞} for the Inner Core (Configuration 1), Calculated Using ENDF/B-VI Data, and Their Percent Increase Compared to the JEF-1.1 Values . . . 20

4 Inner Core Fission Production Rates for Configuration 1, Calculated Using JEF-1.1 Data, and Their Deviations from the Mean Benchmark Values . . . 21

5 Inner Core Fission Production Rates for Configuration 1, Calculated Using ENDF/B-VI Data, and Their Percent Increase Compared to the JEF-1.1 Values . . . 21

6 Inner Core Capture Reaction Rates for Configuration 1, Calculated Using JEF-1.1 Data, and Their Deviations from the Mean Benchmark Values . . . 22

7 Inner Core Capture Reaction Rates for Configuration 1, Calculated Using ENDF/B-VI Data, and Their Percent Increase Compared to the JEF-1.1 Values . . . 23

8 Inner Core Fission Reaction Rates for Configuration 1, Calculated Using JEF-1.1 Data, and Their Deviations from the Mean Benchmark Values . . . 24

9 Inner Core Fission Reaction Rates for Configuration 1, Calculated Using ENDF/B-VI Data, and Their Percent Increase Compared to the JEF-1.1 Values . . . 24

10 Neutron Balance Parameters for Configuration 1, Calculated Using JEF-1.1 Data, and Their Deviations from the Mean Benchmark Values . . . 25

11 Neutron Balance Parameters for Configuration 1, Calculated Using ENDF/B-VI Data, and Their Percent Increase Compared to the JEF-1.1 Values . . . 25

12 Breeding and Conversion Ratios by Region, for Configuration 1, Calculated Using JEF-1.1 Data, and Their Deviations from the Mean Benchmark Values . . . 26

13 Breeding and Conversion Ratios by Region, for Configuration 1, Calculated Using ENDF/B-VI Data, and Their Percent Increase Compared to the JEF-1.1 Values 26
14 Central Reaction Rate Ratios per Atom and Centroid of the Central Flux Spectrum (in keV) for Configuration 1, Calculated Using JEF-1.1 Data, and Their Deviations from the Mean Benchmark Values 27
15 Central Reaction Rate Ratios per Atom and Centroid of the Central Flux Spectrum (in keV) for Configuration 1, Calculated Using ENDF/B-VI Data, and Their Percent Increase Compared to the JEF-1.1 Values 27
16 Region Sodium Void Reactivity Worths Calculated Using JEF-1.1 Data, and Their Deviations from the Mean Benchmark Values 28
17 Region Sodium Void Reactivity Worths Calculated Using ENDF/B-VI Data, and Their Percent Increase Compared to the JEF-1.1 Values 28
18 Central Reactivity Worths Expressed in $\delta k_{eff}/k_{eff}/(10^{31}$ Atoms) Calculated Using JEF-1.1 Data, and Their Deviations from the Mean Benchmark Values 29
19 Central Reactivity Worths Expressed in $\delta k_{eff}/k_{eff}/(10^{31}$ Atoms), Calculated Using ENDF/B-VI Data, and Their Percent Increase Compared to the JEF-1.1 Values 29
20 Isothermal Core Fuel Doppler Reactivities, Calculated Using JEF-1.1 Data, and Their Deviations from the Mean Benchmark Values 30
21 Isothermal Core Fuel Doppler Reactivities, Calculated Using ENDF/B-VI Data, and Their Percent Increase Compared to the JEF-1.1 Values 30
22 Reactivity Worths of the Central Control Rod, Calculated Using JEF-1.1 Data, and Their Deviations from the Mean Benchmark Values 31
23 Reactivity Worths of the Central Control Rod, Calculated Using ENDF/B-VI Data, and Their Percent Increase Compared to the JEF-1.1 Values 31
24 Effective Delayed Neutron Fraction β_{eff} and Inhour of Reactivity for Configuration 1, Calculated Using JEF-1.1 Data, and Their Deviations from the Mean Benchmark Values 32
25 Effective Delayed Neutron Fraction β_{eff} and Inhour of Reactivity for Configuration 1, Calculated Using ENDF/B-VI Data, and Their Percent Increase Compared to the JEF-1.1 Values 32
26 Breeding Gains for Configuration 1, Calculated Using JEF-1.1 Data, and Their Deviations from the Mean Benchmark Values 33
27 Central One-Group Cross-Sections for Configuration 1, Collapsed over the Central Flux Spectrum, Calculated Using JEF-1.1 Data, and Their Deviations from the Mean Benchmark Values 33
28 Isotopic Components of Neutron Balance Parameters for the Inner Core of Configuration 1, Calculated Using JEF-1.1 Data, and Their Deviations from the Mean Benchmark Values 34
29 Eigenvalues k_∞ for the Inner Core (Configuration 1), Calculated Using ENDF/B-VI Data, and Their Percent Increase Due to the Use of JEF-1.1 Data for Individual Nuclides 35
30 Eigenvalues k_∞ for the Inner Core (Configuration 1), Calculated Using ENDF/B-VI Data, and Their Percent Increase Due to the Use of JEF-1.1 Data for Individual Reactions, for Relevant Nuclides 36

List of Figures

1 33 Group Fast ^{239}Pu Fission Production Cross Section 37
2 33 Group Fast ^{239}Pu Fission Cross Section 38
3 33 Group Fast Nubar for ^{239}Pu 39
4 33 Group Fast ^{238}U Inclastic Scattering Cross Section 40
5 33 Group Fast ^{23}Na Inclastic Scattering Cross Section 41

1 INTRODUCTION

Results of an international calculation of a large (1250 MWe) sodium-cooled fast breeder reactor benchmark model (LMFBR benchmark) were presented and discussed at a specialist's meeting at Argonne National Laboratory (ANL) in February 1978. Sixteen solutions from ten different participating countries were analyzed and published in a ANL report [1]. The purpose of that exercise, the first detailed comparison for a large commercial sized LMFBR system, was to evaluate and document the agreement and differences in the calculation of key LMFBR physics and safety parameters as a function of different data sets and processing codes.

In 1990 a series of calculations of the LMFBR benchmark model were performed at the Paul Scherrer Institute (PSI) [2] using nuclear data from Revision 1 of the Joint European File (JEF-1.1) [3].

The results, which did not include kinetic parameters, were showing good agreement, generally within one standard deviation, with the average values over the sixteen benchmark solutions.

However, the conversion and breeding ratios were rather small, and the Doppler-reactivity coefficient differed by about four standard deviations compared with the average values over the benchmark solutions.

The main reason for these differences was never completely understood. However, we found a likely explanation in the methodology used for calculating sigma-zero in the Goldstein-Cohen intermediate resonance absorption shielding method (IR method) applied in the whole energy range below 20 MeV.

We therefore decided to recalculate the LMFBR benchmark using shielded cross sections from MICROX-2 [4], an integral transport theory spectrum code originally developed for the efficient and rigorous preparation of broad group neutron cross sections for fast breeder reactors, which explicitly solves the neutron slowing down and thermalization equations on a detailed energy grid for a two region lattice cell.

In this study, we systematically used the newest nuclear data files released, ENDF/B-VI [5] and JEF-1.1, and we additionally performed first-order perturbation-theory calculations with a PSI version of the code PERT-V [6].

The main objectives for this study were the further testing of the capability and the adequacy of PSI codes for typical "clean" fast reactor configurations, the resolution of the above-mentioned problem with the Doppler-reactivity coefficient (at PSI), and the identification of relevant discrepancies coming from the use of two different, modern nuclear data sources.

In Section 2 of this report the new JEF-1.1 and ENDF/B-VI data libraries for the cell code MICROX-2, including their processing scheme based on the NJOY code system (Version 89.62), are presented.

Section 3 is devoted to the explanation of the main features of the cell code MICROX-2 and to the description of the PSI version of the first-order perturbation-theory code PERT-V.

Section 4 deals with the computational model used,

Section 5 reports on the main results, and Section 6 gives conclusions and recommendations.

2 NUCLEAR DATA

All calculations were performed using new ENDF/B-VI and JEF-1.1 based cross section libraries in FDTAPE, GARTAPE, and GGTAPE format, for the cell code MICROX-2, and microscopic group delayed neutron precursor data files DLAYXS [7] for the first-order perturbation theory code PERT-V.

2.1 NJOY Libraries

Pointwise neutron cross sections in the ENDF/B like format PENDF have been prepared for the nuclides required in the LMFBR benchmark using the modules RECONR, BROADR, UNRESR, and THERMR of a new release of NJOY (Version 89.62), which includes all updates of Version 89.0 up to June 1990 [8], and a modification in RECONR to the p-wave capture in ENDF/B-VI structural materials suggested by Eaton and Rowlands [9,10].

The RECONR module reconstructs pointwise (energy-dependent) zero temperature cross sections using ENDF/B resonance parameters and interpolation schemes. Resonance cross sections are calculated with an extended version of the methods of RESEND [11].

BROADR Doppler-broadens and thins pointwise cross sections using the method of SIGMA modified for better behaviour at high temperatures and low energies [12].

UNRESR computes effective self-shielded energy-, but not yet group-averaged cross sections in the unresolved-resonance region using the methods of ETOX [13].

RECONR (Version 89.62) now is able to use the more sophisticated Reich Moore formalism for treating the resolved energy range.

The PENDF files were generated using the JEF-1.1 and ENDF/B-VI evaluations.

The JEF-1.1 PENDF files consist of data for ^{10}B, ^{11}B, ^{12}C, ^{16}O, ^{23}Na, natural chromium, iron, and nickel, ^{55}Mn, ^{235}U, ^{238}U, ^{239}Pu, ^{240}Pu, ^{241}Pu, ^{242}Pu, at 1100 K, and for ^{16}O, ^{235}U, ^{238}U, ^{239}Pu, ^{240}Pu, ^{241}Pu, and ^{242}Pu at 2200 K respectively.

The ENDF/B-VI PENDF files were processed for the same nuclides and temperatures as for JEF-1.1 except for the structural materials. The individual isotopes of chromium, i.e. ^{50}Cr, ^{52}Cr, ^{53}Cr, ^{54}Cr, of iron, i.e. ^{54}Fe, ^{56}Fe, ^{57}Fe, ^{58}Fe, and of nickel, i.e. ^{58}Ni, ^{60}Ni, ^{61}Ni, ^{62}Ni, ^{64}Ni were generated, since there is no ENDF/B-VI data available for the natural structural elements.

Data for natural molybdenum was processed from JEF-2.0 due to some difficulties encountered in NJOY when processing JEF-1.1 or ENDF/B-VI. Since the absorption in molybdenum is small compared to the total absorption, the substitution of JEF-2.0 cross sections for molybdenum has a negligible effect.

A PENDF file containing data for the inverse neutron velocities was produced from a pseudo JEF-1.1 nuclide generated at PSI using RECONR.

ENDF/B-VI and JEF-1.1 multigroup neutron cross sections in the GENDF format were generated from each PENDF file (including the PENDF file for the inverse velocities) with the GROUPR module, using the 193 neutron group structure from General Atomics [14]. The boundaries of the first 92 fast energy groups of the 193 neutron group structure used in MICROX-2 are taken from the GAM-II

energy structure, whereas in the thermal range below 2.38 eV the boundaries coincide with the energy points of the MICROX code. The 92 fast energy group structure has 63 energy groups above 3.35 keV, i.e. 49 groups with lethargy width 0.10, followed by 14 groups with lethargy width 0.25.

In addition, JEF-1.1 GENDF files in 33 neutron groups were produced for ^{235}U, ^{238}U, ^{239}Pu, ^{240}Pu, and ^{241}Pu, and combined into a single GENDF file for use in obtaining 33 group delayed neutron precursor data DLAYXS.

In a similar way a GENDF file was generated including ENDF/B-VI data for the required actinides ^{235}U, ^{238}U, ^{239}Pu, ^{240}Pu, ^{241}Pu, and ^{242}Pu.

The 33 neutron group structure, a subset of the 193 neutron groups, consists of a top group between 10 and 14.92 MeV, of 30 groups with constant lethargy width 0.5 between 10 MeV and 3.06 eV, and of two additional bottom groups between 3.06 and 2.38 eV, and 2.38 eV and 0.5 meV respectively, the group boundary at 2.38 eV being required in the MICROX-2 calculations.

The built-in input spectrum for fast breeder calculations (i. e. IWT=7 in the GROUPR terminology) was used for generating the multigroup cross sections.

The new automatic vector and matrix reaction options in GROUPR (i.e. 3/, 6/) were used except for some fissionable isotopes (such as ^{235}U in ENDF/B-VI), where there are still some inconsistencies in the availability of the fission reactions on the Files 3, 4, and 5 (in ENDF/B terminology).

GROUPR generates self-shielded groupwise vector cross sections, group-to-group neutron scattering matrices and photon production matrices using pointwise ENDF and PENDF data. The cross sections are written onto groupwise cross section files GENDF in ENDF/B like format [15]. Vectors for all reaction types, matrices for reactions producing neutrons, including fission together with mixed data pertaining to fission yields of prompt and delayed neutrons can be generated.

The GROUPR format data sets in 193 neutron groups consist of shielded vector cross sections and P_0 through P_4 scattering matrices for all reaction types available on the PENDF files, which include double-differential scattering ENDF/B-VI cross sections in energy and angle (File 6 in ENDF/B terminology), and prompt and delayed fission, when appropriate. In addition, they contain data for the average cosine of the scattering angle, for the average energy decrement, and for the average square energy decrement (MT=251, 252, 253 in ENDF/B terminology).

Shielding factors were calculated in GROUPR using the narrow-resonance Bondarenko flux model. These refer to the isotope dependent sigma-zero tabulation given in Table 1. The sigma-zero values from Table 1 were empirically defined based on existing experience with fast breeder reactor calculations [16].

The GROUPR format data sets in 33 groups for the required actinides consist of infinitely dilute (sigma zero is equal to 10^{10} barns) vector cross sections and P_0 through P_1 scattering matrices, including prompt and delayed fission. ^{242}Pu from JEF-1.1 could not be processed because there is no ^{242}Pu delayed neutron data available in JEF-1.1.

2.2 MICROX-2 Libraries

GENDF files in 193 neutron groups and PENDF data files can be edited into the FDTAPE, GGTAPE and GARTAPE input files for MICROX-2 using the coupling and reformatting module MICROR [17] (Version 2) developed and maintained at PSI.

Isotope	Sigma-Zero Values (barns)
^{10}B	10^{10}
^{11}B	10^{10}
^{12}C	10^{10}
^{16}O	10^{10}
^{23}Na	10^{10} 100 20
Cr-isotopes	10^{10} 100 1
^{25}Mn	10^{10} 1000 1
Fe-isotopes	10^{10} 100 50 20
Ni-isotopes	10^{10} 1000 1
Monat	10^{10} 1000 1
^{235}U	10^{10} 1000
^{238}U	10^{10} 1000 100 20
^{239}Pu	10^{10} 1000 100
^{240}Pu	10^{10} 10^{4} 1000 100
^{241}Pu	10^{10}
^{242}Pu	10^{10}

Table 1: Sigma-Zero Values by Isotope in the GENDF Data Files

Corrections to an older version of the MICROR code (Version 1) used in a previous study [18] were applied to allow the FDTAPE and GGTAPE libraries to include an unlimited number of data sets (there was a limit of 50), and to eliminate an error leading to an unexpected truncation of the inelastic outscatter vectors particularly affecting ^{238}U ENDF/B-VI fast data. Variable dimensions and consistent common blocks were introduced and replaced most of the fixed dimensions, especially in the GGTAPE section of the code.

The FDTAPE data file contains fine group dilution- and temperature- dependent cross sections in the fast energy range.

The GGTAPE data file consists of two sections which include infinitely dilute P_0 and P_1 cross sections in the fast and thermal energy ranges respectively.

The GARTAPE data library contains pointwise, Doppler-broadened capture, fission, fission production (ν times σ_f), and elastic scattering resonance cross sections. Fine points up to about 9 keV, the threshold energy for ^{235}U inelastic scattering, may be defined according to the criterium of equidistant lethargy or velocity spacing to be used in MICROX-2 for an accurate self-shielding of the resolved resonance range as a solution of slowing down equations in two zones.

Starting from the GENDF data in 193 groups and from the PENDF files described in the previous section, ENDF/B-VI and JEF-1.1, FDTAPE, GGTAPE, and GARTAPE data libraries suited for fast breeder reactor calculations were generated. In addition, FDTAPE, GGTAPE, and GARTAPE libraries were generated which contain cross sections from both the ENDF/B-VI and JEF-1.1 evaluations.

The FDTAPE data sets include 92 neutron group self-shielded cross sections up to P_3. Individual fission spectra for the actinides ^{235}U, ^{238}U, ^{239}Pu, ^{240}Pu, ^{241}Pu, and ^{242}Pu, calculated in MICROR according to the methodology described in [19], were included in the FDTAPE and GGTAPE libraries.

The GARTAPE data libraries were generated on the basis of equidistant velocity spacing which results in a larger density of points at higher energies compared to the equidistant lethargy spacing, and the tabulation includes 11982 energy points between 2 eV and 2 keV.

2.3 Delayed Neutron Libraries

The JEF-1.1 and ENDF/B-VI GENDF files in 33 neutron groups were edited and reformatted into microscopic group delayed neutron precursor data DLAYXS for the first-order perturbation theory code PERT-V using the NJOY module CCCCR, and converted to binary form using a management code developed for internal use at PSI [20]. The DLAYXS format provides precursor yields, emission spectra, and decay constants ordered by isotope. Isotopes are identified by absolute isotope labels.

3 CODES

The required cell calculations were performed with a PSI version (Edition 14) of the cell code MICROX-2 from General Atomics, the inner core k_∞ calculations with the one-dimensional discrete-ordinates transport code ONEDANT [21], the full reactor forward and adjoint calculations with the two-dimensional discrete-ordinates transport theory code TWODANT from Los Alamos [21], and the perturbation theory calculations with a PSI version of the first-order perturbation theory code PERT-V from Battelle-Northwest obtained from Los Alamos [22].

3.1 MICROX-2

MICROX-2 is an integral transport theory spectrum code which solves the neutron slowing down and thermalization equations on a detailed energy grid for a two region lattice cell. It was developed for the efficient and rigorous preparation of broad group neutron cross sections for poorly moderated systems such as fast breeder reactors as well as for well moderated thermal reactors such as high temperature reactors and light water reactors.

Estimates for the cell eigenvalues (k_{eff} and k_{∞}) are made, and reaction rates can be calculated in a variety of broad group structures.

The fluxes in the two regions are coupled by transport corrected collision probabilities for the generation of the region-wise transfer probabilities in the fast- and resonance-energy ranges. The computation of these collision probabilities is based on the spatially flat neutron emission approximation, on the transport approximation of anisotropic scattering (modified P_0), and on an energy dependent Dancoff correction factor algorithm. The slowing down calculation is performed on an ultra-fine energy grid using the GARTAPE data library.

In Edition 14 of the code, an input value smaller than the maximum energy available on the GARTAPE file determines the upper energy boundary for the pointwise resonance calculation.

Shielded, Doppler-broadened cross sections in the fast and unresolved energy ranges above the chosen input energy can be generated using a semi-logarithmic interpolation of the Bondarenko type between two FDTAPE input data sets.

P_0 through P_3 scattering cross sections in the fast energy range (FDTAPE data library) are considered.

The neutron leakage is determined by performing fine group and hyperfine point B_1 slowing down in the fast and resonance-energy ranges.

Input energy-dependent bucklings (positive, zero, or negative) can be supplied, and a buckling search as a solution of the collapsed (with the fine flux) two group B_1 equations can be turned on.

Two levels of heterogeneity can be treated. The inner region may include two different types of grains (particles).

Regionwise fission spectra may be specified as mixtures of fission spectra for the single actinides available on the FDTAPE data library.

Due to the high resolution of the energy points in the GARTAPE data library, MICROX-2 explicitely accounts for overlap and interference effects between different resonance levels. In addition, leakage and resonance self-shielding in doubly heterogeneous lattice cells can be treated simultaneously.

For the preparation of adequate groupwise cross sections the buckling search may be activated.

The detailed neutron flux and current spectra are used for collapsing GARTAPE, FDTAPE, and GGTAPE library cross sections into cell-averaged and region-averaged broad-group microscopic and macroscopic cross sections and scattering transfer arrays (up to P_1).

Broad group P_2 and P_3 scattering transfer arrays may be determined with P_2 and P_3 weighting

spectra obtained from an extended transport approximation.

The broad group cross sections (macroscopic and microscopic) may be used in the transport-theory codes ONEDANT and TWODANT and subsequently in a PSI version of the first-order perturbation theory code PERT-V via an XSLIB output format, one of the simplest Los Alamos card image formats [21].

3.2 ONEDANT and TWODANT

ONEDANT is a modular computer program designed to solve the one-dimensional, time-independent, multigroup discrete-ordinates form of the Boltzmann transport equations, using a finite-difference discretization scheme. The modular construction of the code package separates the input processing, the transport equation solving, and the post-processing, or edit, functions into distinct, independently executable code modules, connected to one another solely by means of binary interface files.

TWODANT is the analog of ONEDANT in two dimensions.

3.3 PERT-V

PERT-V is a first-order perturbation theory code originally developed at the Battelle-Northwest Laboratory for sodium-cooled, fast breeder reactor analyses, and subsequently modified at the Los Alamos National Laboratory to accept input data from standard interface files [7]. PERT-V is designed to compute the effective delayed neutron fraction, the neutron generation time and the conversion factor between inhours and delta-k, to compute reactivity coefficients, and to perform activity edits, including eigenvalues and reaction rates.

The leakage components of the reactivity coefficients are computed with a mesh-centered diffusion theory finite-difference approximation. The other components of the reactivity coefficients, the effective delayed neutron fraction, the neutron generation time, the inhour/delta-k conversion factor, and the activities are computed directly from the broad-group direct and adjoint fluxes and cross sections supplied to the PERT-V code.

The required direct and adjoint fluxes can be obtained from RTFLUX and ATFLUX, and from the geometrical and atom density standard files GEODST, NDXSRF, and ZNATDN [7] prepared by ONEDANT and TWODANT.

The PSI-version of the PERT-V code [23] includes the following new capabilities as compared with the Los Alamos version, namely a multithermal-group (up-scatter) capability, an XSLIB format cross section input file option (microscopic cross sections for each isotope to be perturbed must be available on XSLIB), a computation of DB^2 terms after the zone-dependent buckling modifiers are read instead of before, corrections to prevent the use of variables before they are initialized, FORTRAN-77 list-directed (free field) user input formats, a cross section balance test, an explicit edit of the (n,2n) reactivity coefficient component when the required (n,2n) cross section data is available, an option to control the addition of the (n,2n) component into the total reactivity coefficient, various corrections to check additional parametrized dimensions, and a revised β_{eff} and inhour equation coding for multi-isotope systems.

4 COMPUTATIONAL MODEL

The benchmark reactor specifications described in detail in Ref. 1, are based on a 3260 MWt (1250 MWe) conventional mixed oxide design for a large (1250 MWe) LMFBR model. The benchmark model was set up for (r,z) modeling with specified homogeneous compositions for each region of the reactor. The core height is 101.6 cm, the radii of the inner and outer core regions are 136.85 and 176.53 cm, respectively, giving a total core volume of 9950 liters. The core volume fractions are 41 % for fuel, 38 % for total sodium, and 21 % for total structural material.

Eight configurations to be calculated were specified, namely the reference configuration (Configuration 1), a Na-voided inner core configuration (Configuration 2), a Na-voided inner core, outer core and axial blanket configuration (Configuration 3), the reference configuration with a central Na-filled control rod position (Configuration 4), the reference configuration with a central boron control rod (Configuration 5), a configuration with the Na-voided inner core, outer core and axial blanket with a central boron control rod (Configuration 6), the reference configuration with hot fuel (Configuration 7), and and a configuration with the Na-voided inner core, outer core, and axial blanket with hot fuel (Configuration 8).

The performance parameters calculated in this study (see Ref. 1, pages 160-171) include k_{eff} values for the eight configurations, k_∞ for the inner core composition, neutron balance data, the centroid of the central flux spectrum for Configuration 1 (an average neutron energy, as defined in Ref. 1, page 13), global and regional breeding and conversion ratios, breeding gains (see Ref. 1, pages 166-167), central reaction rate ratios and reactivity worths with and without sodium, effective one-group cross sections, effective delayed neutron fraction β_{eff} and inhour reactivity, regional sodium void reactivity, and isothermal core fuel Doppler-reactivities.

To make a direct comparison with previously published results, the model described in Ref. 1, including geometry, number of meshes in each direction, and cross section preparation scheme, was followed as closely as possible, except that modified P_0 S_4 transport theory was used instead of diffusion theory.

We defined a two-dimensional (r,z) geometry with axial symmetry about the vertical axis with a vacuum boundary condition at the outside boundary of the reflector region, and we decreased the original reflector thickness by the extrapolation distance in the reflector (i.e. by 1.37 cm). As in the previous study done at PSI [2] the resulting eigenvalues were multiplied with a conversion factor equal to 0.99872 [1], to account for the difference between transport and diffusion theory. We calculated reaction rates and reactivity worths at the reactor centre by considering a central, additional thin zone, of 0.01 cm x 0.01 cm.

Homogeneous cell calculations in the fundamental mode (i.e. the critical buckling was searched for) were performed in the inner core and outer core regions. We did further cell calculations with a zero buckling in the inner core region to generate cross sections to be used for determining the eigenvalue k_∞ for the inner core composition.

In the blanket regions we used a zero buckling, and made fixed source slowing down (cell) calculations with a pure fission source for ^{239}Pu as the source.

We used radial blanket cross sections for the reflector region.

There are two criteria for adequately defining the upper energy limit for the slowing down calculation in Edition 14 of the MICROX-2 code [24].

First, it should match a fine, and possibly a coarse group boundary, at which the moderator cross section does not vary too rapidly as a function of energy. Only in this way FDTAPE and GARTAPE cross sections are used in a consistent way when the slowing down equation is initialized. Edition 14 of MICROX-2 automatically redefines this input value if it does not match a fine group boundary.

Second, this energy limit should be smaller than the minimum energy of the break between resolved and unresolved range over all important isotopes involved, such that the unresolved resonance range can be shielded using the Bondarenko formalism.

This condition is needed because the unresolved resonance cross sections presently available on the GARTAPE data library, coming from a sigma-zero tabulation originally done in UNRESR and obtained by averaging the cross sections over the unresolved resonance parameters, are energy-averaged cross sections given at infinite dilution [17].

The upper limit for the pointwise slowing down calculations was set at 582.947 eV in all cell calculations, corresponding to the upper energy boundary for fine group 71 in the 193 group structure. This energy coincides with the first fine group boundary below the upper bound of the resolved resonance range for ^{239}Pu in JEF-1.1 (i.e. 598 eV), at which the sodium cross section is almost energy independent.

The unresolved energy ranges for ^{235}U and ^{241}Pu, which start at lower energies (i.e. at 82 eV and 100 eV in JEF-1.1), do not need to be shielded, because ^{235}U and ^{241}Pu are almost at infinite dilution in this problem.

582.947 eV does not coincide with a coarse group boundary. However, the choice of the first possible coarse group boundary below 598 eV (i.e. 454 eV) would significantly reduce the number of energy points accounted for in the slowing down calculation.

Therefore, using this version of MICROX-2 it is not possible to include the main sodium resonance (occurring at about 2.5 keV) in the pointwise calculation.

This is the main reason why pointwise cross sections above 2 keV were not included in the GARTAPE data library.

The extension of the resolved resonance range for ^{239}Pu in ENDF/B-VI to 2 keV is within this context of no significant help, because of the strong variation of the sodium cross section between 2 and 7 keV.

Different 33 neutron broad group, P_0 modified cross sections were generated for each of the eight compositions to account for the spatial dependence of the spectrum and separate sets for high temperature fuel were specified for a Doppler-coefficient calculation: seven sets of broad group isotopic microscopic cross sections including groupwise inverse velocities for use in PERT-V, and macroscopic cross sections were prepared by collapsing (in MICROX-2) fine group sets (from the FDTAPE, GARTAPE, and GGTAPE data libraries) over the spectra calculated from the different homogeneous cell calculations.

In these sets all isotopes were assumed to be at a temperature of 1100 K. Four additional sets of broad group isotopic microscopic, and macroscopic cross sections for the calculation of the Doppler-coefficient were generated at 2200 K for the isotopes ^{235}U, ^{238}U, ^{239}Pu, ^{240}Pu, ^{241}Pu, ^{242}Pu, and ^{16}O,

and at 1100 K for all other isotopes.

The regionwise fission spectra were calculated as linear combinations of library fission spectra unless otherwise specified. The fractions for each actinide, determined by a first series of homogeneous cell calculations in the fundamental mode with a pure ^{239}Pu fission source, was the ratio between the actinide and the total fission production rate in each cell.

The resulting fission spectra were found to be almost independent of the zone and configuration considered, and can approximately be expressed as the sum of the fission spectrum for ^{239}Pu multiplied with 0.7, of that for ^{241}Pu multiplied with 0.16, and of the fission spectrum for ^{238}U multiplied with 0.14. It appears that the calculated parameters are only weakly dependent on the fission spectrum used.

The required isotope dependent maximum and minimum dilution cross section values over the fast and unresolved energy ranges needed for shielding these energy ranges were determined by a series of cell calculations, in which an energy independent dilution cross section was estimated in a first and crude approximation as the ratio between one-group macroscopic cross section of an homogeneous mixture consisting of all remaining cell isotopes, and atom density of this isotope in the cell.

The calculated parameters were found not to be too sensitive to the FDTAPE input data sets chosen, if the interpolation range is not too wide and does include the maximum and minimum sigma-zero values.

Transport-theory calculations (forward and adjoint), and first-order perturbation-theory calculations were performed using the 33 neutron group structure described in the previous section, which includes six additional groups compared to the group structure referenced in [1], i.e. the top group between 10 and 14.92 MeV, and the five groups below 13.71 eV.

Cell and transport-theory calculations were performed using ENDF/B-VI data for each isotope of the structural materials. 33 group ENDF/B-VI cross sections for the natural structural materials only were constructed for use in the perturbation-theory calculations to determine the central reactivity worth for natural iron.

In the TWODANT calculations excellent agreement within 0.01 % was achieved in the calculated eigenvalues k_{eff} between forward and adjoint calculation, and between calculations done either with macroscopic zonewise cross sections or with microscopic cross sections homogenized over each zone in the transport-theory calculation itself.

The input convergence parameter EPSI [21] was set to 10^{-5}. The choice of a smaller value than the default value (i.e. 10^{-4}) is particularly important in view of an accurate prediction of the Doppler-coefficient, which is small in magnitude compared to the eigenvalue (i.e. about 0.7% of the k_{eff} value).

In the PERT-V calculations with JEF-1.1 cross sections, we used ^{240}Pu delayed data for ^{242}Pu (see previous section). However, the contribution to β_{eff} due to ^{242}Pu was found to be minor. The fission spectrum used was that for the inner core region.

The non-buckled eigenvalue k_∞ for the inner core composition (for Configuration 1) was calculated using ONEDANT and a one-zone infinite cell model in slab geometry. The relative difference of the computed eigenvalues k_∞ between MICROX-2 and ONEDANT was found to be about 0.35%, the ONEDANT eigenvalue being larger than the MICROX-2 eigenvalue.

Throughout the report
C8 denotes the $^{238}U(n,\gamma)$,
F8 the ^{238}U(n,fission) reaction rate per atom of ^{238}U,
C9 the $^{239}Pu(n,\gamma)$,
and F9 the ^{239}Pu(n,fission) reaction rate per atom of ^{239}Pu.

$k_{Bsquared}$ is the ratio between fission production and absorption rate in the core.

5 RESULTS AND DISCUSSION

Tables 2-28 summarize the results obtained using JEF-1.1 data, their relative deviations from the mean benchmark values, and the standard deviations calculated from the sixteen benchmark solutions presented in Ref. 1.

In addition, they summarize the corresponding, most important results obtained using ENDF/B-VI data, and their variations relative to the JEF-1.1 values.

Each table can be identified through the same convention as adopted in the original report [1] (i.e. Table D1 refers to the summary of the calculated eigenvalues).

Tables 2-28 prove that the new results generally lie within one standard deviation of average benchmark values.

Specific differences between the ENDF/B-VI and JEF-1.1 results include:

- The eigenvalues k_{eff} for the eight configurations predicted with ENDF/B-VI are up to 0.7% larger than those calculated with JEF-1.1 (see Tables 2, 3).
- The eigenvalue k_∞ for the inner core of Configuration 1 significantly increases by 1.38 % when using ENDF/B-VI cross sections (i.e. 1.134 versus 1.119).
- Tables 10-13 show that the breeding ratio in the core increases by 2.20 % (i.e. 0.988 versus 0.967), that in the blanket region by 5.35 % (i.e. 0.419 versus 0.397), the reactor breeding ratio by 3.11 % (i.e. 1.407 versus 1.364), the conversion ratio in the inner core by 1.48 % (i.e. 1.084 versus 1.068), that in the outer core region by 1.34 % (i.e. 0.811 versus 0.800), and the total neutron leakage by 10.53 % (i.e. 0.0173 versus 0.0156).
- The centroid of the central flux spectrum increases by 8.09 % (i.e. 112.8 versus 104.3 keV), and the ratio between C8 and F9 evaluated at the core centre by 4.83 % (i.e. 0.170 versus 0.162). The ratio between C9 and F9 decreases by 5.33 % (i.e. 0.297 versus 0.314) when using ENDF/B-VI cross sections (see Tables 14, 15).
- The region sodium void reactivity worth for the inner core calculated with ENDF/B-VI is 5.81 % smaller (i.e. 0.0218 versus 0.0231), and that for the core and axial blanket is 5.31 % smaller (i.e. 0.0229 versus 0.0242), than the corresponding JEF-1.1 values (see Tables 16, 17).
- The reactivity worth of the central control rod with sodium relative to the fuel increases by 7.44 % (i.e. -0.00361 versus -0.00336), that relative to the sodium-filled control rod position by 7.80 % (i.e. -0.00304 versus -0.00282), and the reactivity worth of the central control rod without sodium relative to the fuel by 3.63 % (i.e. -0.00455 versus -0.00439) when using ENDF/B-VI cross sections (compare Tables 22, 23).

- The isothermal core fuel Doppler-reactivity coefficient (see Tables 20-21) agreed well within slightly more than one half of a standard deviation with the mean benchmark value. This is in contrast to the previous study done at PSI [2]. The ENDF/B-VI value overestimates the JEF-1.1 value by 1.50 % for Configuration 1 (i.e. -0.00751 versus -0.00740), and by 8.58 % for Configuration 3 (i.e. -0.00430 versus -0.00396).

- The effective delayed neutron fraction for Configuration 1 is 2.65 % larger (i.e. 0.00392 versus 0.00382), and the inhour of reactivity 5.04 % smaller (i.e. 1.082×10^{-5} versus 1.140×10^{-5}) when using ENDF/B-VI data (see Tables 24, 25).

- Tables 18 and 19 show that there are no significant differences between JEF-1.1 and ENDF/B-VI in the calculation of the central reactivity worths except for sodium. The rather big sodium worth in Configuration 3, calculated with JEF-1.1 data (about 1.3 standard deviations larger than the mean benchmark value), significantly decreases (by about 0.5 standard deviations) when using ENDF/B-VI cross sections (i.e. -1.08×10^{-6} versus -1.01×10^{-6} $\delta k_{eff}/k_{eff}/(10^{24}$ atoms)).

- Tables 4-9 show that there are considerable differences between these two evaluations in the fast fission, fission production, and capture cross sections for ^{240}Pu and ^{242}Pu, and in the fast capture cross sections for ^{241}Pu, ^{16}O, ^{23}Na, chromium, and ^{55}Mn.

- Figures 1-2 show that the fast fission and fission production cross sections of ^{239}Pu between 10 keV and 1 MeV are up to 6 % larger in JEF-1.1 than in ENDF/B-VI. The maximum differences occur at about 50 keV (1.6 versus 1.5, respectively 4.7 versus 4.4 barns).

- Figure 3 shows that nubar for ^{239}Pu at energies between 10 keV and about 300 keV is systematically smaller by almost 1 % in JEF-1.1 than in ENDF/B-VI.

- Figure 4 indicates that the inelastic scattering ENDF/B-VI cross section for ^{238}U is significantly, up to 100 %, larger than the JEF-1.1 cross section at energies between 1 and 10 MeV. The ENDF/B-VI cross section is up to 15 % larger at energies between 200 and 400 keV (i.e. 1.24 versus 1.07 barns at about 240 keV), whereas it is significantly smaller (by about 30 %) than the JEF-1.1 cross section below 100 keV.

- Figure 5 indicates a considerable discrepancy between JEF-1.1 and ENDF/B-VI in the inelastic scattering cross section for ^{23}Na at energies below 2 MeV (20 % difference at 1 MeV, about 0.55 barns in JEF-1.1, and 0.45 barns in ENDF/B-VI).

- Table 29 shows the relative variation of the eigenvalue k_∞ for the inner core of Configuration 1 when substituting ENDF/B-VI with JEF-1.1 data for individual isotopes. The main contributions to this variation are from ^{239}Pu (+0.78 %), from ^{238}U (-0.99 %), and from ^{23}Na (-0.67 %). Less important contributions are from ^{240}Pu and ^{16}O (-0.22 %), and from iron (-0.13 %).

- In Table 30 ENDF/B-VI cross sections and scattering transfer arrays for ^{239}Pu, ^{238}U, and ^{23}Na were replaced for individual reactions by JEF-1.1 cross sections. The increase of k_∞ due to ^{239}Pu comes primarily from the fission production cross section. However, there are two opposite effects, a strong increase coming from the fission cross section itself (+1.65 %), and a decrease coming from nubar (-0.59 %) and from the capture cross section (-0.31 %). About 85 % and 120 % of the decrease of k_∞ due to ^{23}Na and ^{238}U are from the inelastic scattering data.

6 CONCLUSIONS AND RECOMMENDATIONS

The present analyses dealt with neutronics calculations of a large sodium-cooled fast breeder reactor, performed using data from the ENDF/B-VI and JEF-1.1 evaluations.

The required cross sections were processed with the NJOY code system (Version 89.62) and homogenized in energy with the spectrum cell code MICROX-2. Multigroup transport-theory calculations in 33 groups (forward and adjoint) were performed using the two-dimensional code TWODANT and kinetic parameters were determined using the first-order perturbation-theory code PERT-V.

We calculated eigenvalues, neutron balance data, global and regional breeding and conversion ratios, central reaction rate ratios and reactivity worths, regional sodium void reactivity, isothermal core fuel Doppler-reactivities, effective delayed neutron fraction, and inhour reactivity.

The results were compared with the average values over sixteen solutions obtained in the past.

From this study the following conclusions can be reached, and some recommendations can be made.

- Good agreement generally within one standard deviation was achieved between the new ENDF/B-VI and JEF-1.1 results, and the average values over the sixteen benchmark solutions obtained in the past. In particular, the calculated isothermal core fuel Doppler-reactivity coefficient agreed well (within slightly more than one half of a standard deviation) with the mean benchmark value.

- Although both the JEF-1.1 and ENDF/B-VI evaluations seem to be adequate, we observed considerable differences among them in the energy range important for fast breeder reactor calculations. These refer to the fission of ^{239}Pu, ^{240}Pu, and ^{242}Pu, to the neutron capture in ^{241}Pu, ^{242}Pu, ^{16}O, ^{23}Na, chromium, and ^{55}Mn, and to the inelastic scattering cross section and transfer arrays for ^{238}U and ^{23}Na.

  The eigenvalues k_{eff} for the eight configurations considered, and the eigenvalue k_{∞} for the inner core of Configuration 1 predicted with ENDF/B-VI, were up to 0.7%, respectively 1.38 % larger than those calculated with JEF-1.1, and the central sodium worth in Configuration 3, slightly too big when using JEF-1.1 data, significantly decreased by about 6.5 % (one half of a standard deviation) when using ENDF/B-VI cross sections.

- These discrepancies are mostly coming from ^{239}Pu, ^{238}U, and ^{23}Na. The ^{239}Pu fission production cross section between 10 keV and 1 MeV is up to 6 % larger in JEF-1.1 than in ENDF/B-VI. The ^{238}U ENDF/B-VI inelastic scattering cross section between 1 and 10 MeV is almost twice the JEF-1.1 value, and is about 15 % larger than the JEF-1.1 cross section at energies between 200 and 400 keV. The ^{23}Na ENDF/B-VI inelastic scattering cross section below 2 MeV is up to 20 % smaller than the JEF-1.1 cross section.

- Therefore, we either recommend a new evaluation or a reduction of the uncertainty of these cross sections in the energy range between 10 keV and 1 MeV. Furthermore, the alternative use of JEF-2 data, when officially released, would be valuable; it is recommended to calculate a fast breeder reactor benchmark experiment, and to compare especially the predicted and measured Doppler-reactivity coefficient.

- Either the cell code MICROX-2 (PSI Edition 14) or the module UNRESR of NJOY (Version 89.62), should be modified in such a way that the main sodium resonance at 2.5 keV can be

considered in the detailed pointwise slowing down calculation. The use of an alternative cell code would be valuable.

- Otherwise, the methodology used in MICROX-2 for generating broad group cross sections, consisting of a two-zone pointwise solution of the slowing down equations in the resolved resonance energy range and of an interpolation scheme of the Bondarenko type above, seems to be suitable for fast breeder reactor calculations.

Acknowledgments

The author would like to acknowledge Dr. D. Mathews, Dr. H. U. Wenger, and Dr. P. Wydler for valuable discussions during the execution of this work.

Table D1 Configuration	Eigenvalue	Standard Deviation (%)	Deviation from the Mean Value (%)
Inner Core	1.11890	1.80	-0.48
1	1.01104	1.29	0.59
2	1.03442	1.34	0.78
3	1.03551	1.37	0.91
4	1.01049	1.28	0.59
5	1.00764	1.26	0.61
6	1.03096	1.34	0.90
7	1.00356	1.31	0.57
8	1.03141	1.34	0.94

Table 2: Eigenvalues k_{eff} for the Eight Configurations, Eigenvalue k_{∞} for the Inner Core (Configuration 1), Calculated Using JEF-1.1 Data, and Their Deviations from the Mean Benchmark Values

Table D1 Configuration	Eigenvalue	% Increase Compared to JEF-1.1
Inner Core	1.13438	1.38
1	1.01853	0.74
2	1.04071	0.61
3	1.04187	0.61
4	1.01794	0.74
5	1.01485	0.72
6	1.03713	0.60
7	1.01088	0.73
8	1.03739	0.58

Table 3: Eigenvalues k_{eff} for the Eight Configurations, Eigenvalue k_{∞} for the Inner Core (Configuration 1), Calculated Using ENDF/B-VI Data, and Their Percent Increase Compared to the JEF-1.1 Values

Table D2.a-1	Reaction Rate	Standard Deviation (%)	Deviation from the Mean Value (%)
^{239}Pu	0.418204	1.26	-0.19
^{240}Pu	0.023206	8.17	-1.25
^{241}Pu	0.091630	7.12	-2.50
^{242}Pu	0.002021	6.91	-6.87
^{235}U	0.007591	2.06	-2.43
^{238}U	0.089632	3.74	3.70
Total	0.632284	0.83	-0.07

Table 4: Inner Core Fission Production Rates for Configuration 1, Calculated Using JEF-1.1 Data, and Their Deviations from the Mean Benchmark Values

Table D2.a-1	Reaction Rate	% Increase Compared to JEF-1.1
^{239}Pu	0.419254	0.25
^{240}Pu	0.025116	8.23
^{241}Pu	0.091742	0.12
^{242}Pu	0.002212	9.46
^{235}U	0.007731	1.84
^{238}U	0.089654	0.02
Total	0.635709	0.54

Table 5: Inner Core Fission Production Rates for Configuration 1, Calculated Using ENDF/B-VI Data, and Their Percent Increase Compared to the JEF-1.1 Values

Table D2.a-2	Reaction Rate	Standard Deviation (%)	Deviation from the Mean Value (%)
^{239}Pu	0.045484	6.71	5.68
^{240}Pu	0.013837	19.31	6.44
^{241}Pu	0.006206	9.67	-1.65
^{242}Pu	0.001465	20.63	16.27
^{235}U	0.000965	5.15	-0.52
^{238}U	0.231752	3.04	-1.86
^{16}O	0.001809	19.74	19.01
^{23}Na	0.002097	30.80	-0.62
Fenat	0.012590	24.73	-3.30
Ninat	0.006289	15.36	-3.40
Crnat	0.004365	38.98	-14.07
^{55}Mn	0.002009	10.54	-1.03
Monat	0.003379	25.79	-17.79
Total	0.332247	2.33	-0.85

Table 6: Inner Core Capture Reaction Rates for Configuration 1, Calculated Using JEF-1.1 Data, and Their Deviations from the Mean Benchmark Values

Table D2.a-2	Reaction Rate	% Increase Compared to JEF-1.1
^{239}Pu	0.042828	-5.84
^{240}Pu	0.012540	-9.38
^{241}Pu	0.005089	-18.00
^{242}Pu	0.001354	-7.60
^{235}U	0.000911	-5.62
^{238}U	0.231543	-0.09
^{16}O	0.002268	25.35
^{23}Na	0.001898	-9.49
Fenat	0.011794	-6.32
Ninat	0.006278	-0.17
Crnat	0.003581	-17.95
^{55}Mn	0.001507	-25.00
Monat	0.003386	0.21
Total	0.324977	-2.19

Table 7: Inner Core Capture Reaction Rates for Configuration 1, Calculated Using ENDF/B-VI Data, and Their Percent Increase Compared to the JEF-1.1 Values

Table D2.a-3	Reaction Rate	Standard Deviation (%)	Deviation from the Mean Value (%)
^{239}Pu	0.143388	1.34	0.39
^{240}Pu	0.007744	7.51	0.31
^{241}Pu	0.030863	26.90	3.84
^{242}Pu	0.000662	7.04	-6.76
^{235}U	0.003082	0.94	-3.08
^{238}U	0.032208	3.61	3.70
Total	0.217947	0.76	0.39

Table 8: Inner Core Fission Reaction Rates for Configuration 1, Calculated Using JEF-1.1 Data, and Their Deviations from the Mean Benchmark Values

Table D2.a-3	Reaction Rate	% Increase Compared to JEF-1.1
^{239}Pu	0.142347	-0.73
^{240}Pu	0.008337	7.66
^{241}Pu	0.030923	0.20
^{242}Pu	0.000721	8.87
^{235}U	0.003147	2.11
^{238}U	0.032489	0.87
Total	0.217964	0.01

Table 9: Inner Core Fission Reaction Rates for Configuration 1, Calculated Using ENDF/B-VI Data, and Their Percent Increase Compared to the JEF-1.1 Values

Tables D2.b, D3, D4	Parameter Calculated	Standard Deviation (%)	Deviation from the Mean Value (%)
$k_{Bsquared}$	1.206297	1.64	0.17
Fission Prod. (Core)	0.978642	0.16	0.06
Fission Prod. (Reactor)	1	0	0
Capture (Core)	0.474392	2.74	-0.67
Capture (Reactor)	0.631903	2.26	-0.78
Fission (Core)	0.336886	0.30	0.50
Fission (Reactor)	0.344804	0.23	0.44
Absorption (Core)	0.811278	1.69	-0.18
Absorption (Reactor)	0.976707	1.50	-0.36
Leakage (Core)	0.159610	2.47	-1.53
Leakage (Reactor)	0.015621	15.24	-4.75

Table 10: Neutron Balance Parameters for Configuration 1, Calculated Using JEF-1.1 Data, and Their Deviations from the Mean Benchmark Values

Tables D2.b, D3, D4	Parameter Calculated	% Increase Compared to JEF1.1
$k_{Bsquared}$	1.228691	1.86
Fission Prod. (Core)	0.978192	-0.05
Fission Prod. (Reactor)	1	0
Capture (Core)	0.461191	-2.78
Capture (Reactor)	0.619695	-1.93
Fission (Core)	0.334934	-0.58
Fission (Reactor)	0.343265	-0.45
Absorption (Core)	0.796125	-1.87
Absorption (Reactor)	0.964269	-1.27
Leakage (Core)	0.163833	2.65
Leakage (Reactor)	0.017266	10.53

Table 11: Neutron Balance Parameters for Configuration 1, Calculated Using ENDF/B-VI Data, and Their Percent Increase Compared to the JEF-1.1 Values

Tables D5, D6, D7	Breeding Ratio	Std. Dev. (%)	Dev. from Mean Val. (%)	Conversion Ratio	Std. Dev. (%)	Dev. from Mean Val. (%)
Inner Core	0.68635	4.00	-2.37	1.06784	4.25	-2.27
Outer Core	0.28042	5.30	-2.23	0.80049	4.41	-2.55
Core Subtot.	0.96677	4.25	-2.33	/	/	/
Radial Blkt	0.16932	2.13	-0.99	/	/	/
Axial Blkt	0.22811	2.82	-1.36	/	/	/
Blkt Subtot.	0.39743	2.42	-1.20	/	/	/
Reactor Tot.	1.36420	3.46	-2.01	/	/	/

Table 12: Breeding and Conversion Ratios by Region, for Configuration 1, Calculated Using JEF-1.1 Data, and Their Deviations from the Mean Benchmark Values

Tables D5, D6, D7	Breeding Ratio	% Increase Compared to JEF-1.1	Conversion Ratio	% Increase Compared to JEF-1.1
Inner Core	0.70048	2.06	1.08363	1.48
Outer Core	0.28752	2.53	0.81122	1.34
Core Subtot.	0.98800	2.20	/	/
Radial Blkt	0.17762	4.90	/	/
Axial Blkt	0.24108	5.69	/	/
Blkt Subtot.	0.41870	5.35	/	/
Reactor Tot.	1.40670	3.11	/	/

Table 13: Breeding and Conversion Ratios by Region, for Configuration 1, Calculated Using ENDF/B-VI Data, and Their Percent Increase Compared to the JEF-1.1 Values

Tables D10 and V	Reaction Rate Ratio	Standard Deviation (%)	Deviation from the Mean Value (%)
C8/F9	0.16223	3.71	-2.21
F8/F9	0.02289	3.97	3.29
C9/F9	0.31385	5.81	4.72
Centroid	104.33	3.80	-5.63

Table 14: Central Reaction Rate Ratios per Atom and Centroid of the Central Flux Spectrum (in keV) for Configuration 1, Calculated Using JEF-1.1 Data, and Their Deviations from the Mean Benchmark Values

Tables D10 and V	Reaction Rate Ratio	% Increase Compared to JEF-1.1
C8/F9	0.17007	4.83
F8/F9	0.02328	1.69
C9/F9	0.29711	-5.33
Centroid	112.77	8.09

Table 15: Central Reaction Rate Ratios per Atom and Centroid of the Central Flux Spectrum (in keV) for Configuration 1, Calculated Using ENDF/B-VI Data, and Their Percent Increase Compared to the JEF-1.1 Values

Table D11	Reactivity Worth	Standard Deviation (%)	Deviation from the Mean Value (%)
Inner Core	0.02312	12.10	9.27
Inner Core, Outer Core, Axial Blanket	0.02420	16.80	15.35

Table 16: Region Sodium Void Reactivity Worths Calculated Using JEF-1.1 Data, and Their Deviations from the Mean Benchmark Values

Table D11	Reactivity Worth	% Increase Compared to JEF-1.1
Inner Core	0.02178	-5.81
Inner Core, Outer Core, Axial Blanket	0.02292	-5.31

Table 17: Region Sodium Void Reactivity Worths Calculated Using ENDF/B-VI Data, and Their Percent Increase Compared to the JEF-1.1 Values

Table D12	Conf. 1 Worth	Std. Dev. (%)	Dev. from Mean Val. (%)	Conf. 3 Worth	Std. Dev. (%)	Dev. from Mean Val. (%)
^{239}Pu	1184.951	3.73	-0.17	1337.362	2.63	0.18
^{238}U	-74.16905	4.72	1.41	-77.2040	2.80	1.99
^{23}Na	-7.715605	9.75	11.69	-10.83581	12.87	16.48
Fenat	-9.146503	7.83	2.84	-11.48101	4.92	8.01
^{10}B	-762.1203	5.43	-2.59	-721.4733	4.43	-2.78

Table 18: Central Reactivity Worths Expressed in $\delta k_{eff}/k_{eff}/(10^{31}$ Atoms) Calculated Using JEF-1.1 Data, and Their Deviations from the Mean Benchmark Values

Table D12	Conf. 1 Worth	% Increase Compared to JEF-1.1	Conf. 3 Worth	% Increase Compared to JEF-1.1
^{239}Pu	1221.530	3.09	1340.550	0.24
^{238}U	-75.78510	2.18	-76.58864	-0.80
^{23}Na	-7.530321	-2.40	-10.13490	-6.47
Fenat	-9.097450	-0.54	-11.16548	-2.75
^{10}B	-795.2034	4.34	-741.2405	2.74

Table 19: Central Reactivity Worths Expressed in $\delta k_{eff}/k_{eff}/(10^{31}$ Atoms), Calculated Using ENDF/B-VI Data, and Their Percent Increase Compared to the JEF-1.1 Values

Table D15	Fuel Doppler	Standard Deviation (%)	Deviation from the Mean Value (%)
Configuration 1 Na In	-0.00740	10.80	1.56
Configuration 3 Na Voided	-0.00396	14.30	-8.64

Table 20: Isothermal Core Fuel Doppler Reactivities, Calculated Using JEF-1.1 Data, and Their Deviations from the Mean Benchmark Values

Table D15	Fuel Doppler	% Increase Compared to JEF-1.1
Configuration 1 Na In	-0.00751	1.50
Configuration 3 Na Voided	-0.00430	8.58

Table 21: Isothermal Core Fuel Doppler Reactivities, Calculated Using ENDF/B-VI Data, and Their Percent Increase Compared to the JEF-1.1 Values

Table D16	Reactivity Worth	Standard Deviation (%)	Deviation from the Mean Value (%)
Na In (Relative to Fuel)	-0.00336	13.2	-5.27
Na In (Relative to Na-Filled Control Rod Position)	-0.00282	14.4	-5.46
Na Void (Relative to Fuel)	-0.00439	10.2	-4.58

Table 22: Reactivity Worths of the Central Control Rod, Calculated Using JEF-1.1 Data, and Their Deviations from the Mean Benchmark Values

Table D16	Reactivity Worth	% Increase Compared to JEF-1.1
Na In (Relative to Fuel)	-0.00361	7.44
Na In (Relative to Na-Filled Control Rod Position)	-0.00304	7.80
Na Void (Relative to Fuel)	-0.00455	3.63

Table 23: Reactivity Worths of the Central Control Rod, Calculated Using ENDF/B-VI Data, and Their Percent Increase Compared to the JEF-1.1 Values

Table D17	Reactivity Worth	Standard Deviation (%)	Deviation from the Mean Value (%)
β_{eff}	0.0038227	2.62	-1.16
Inhour of Reactivity	1.1398×10^{-5}	1.62	-1.02

Table 24: Effective Delayed Neutron Fraction β_{eff} and Inhour of Reactivity for Configuration 1, Calculated Using JEF-1.1 Data, and Their Deviations from the Mean Benchmark Values

Table D17	Reactivity Worth	% Increase Compared to JEF-1.1
β_{eff}	0.0039240	2.65
Inhour of Reactivity	1.0823×10^{-5}	-5.04

Table 25: Effective Delayed Neutron Fraction β_{eff} and Inhour of Reactivity for Configuration 1, Calculated Using ENDF/B-VI Data, and Their Percent Increase Compared to the JEF-1.1 Values

Table D18	Reactivity Worth	Standard Deviation (%)	Deviation from the Mean Value (%)
Internal Br. Gain	-0.052643	69.36	13.68
Blanket Br. Gain	0.412424	2.38	0.51
Total Br. Gain	0.359782	9.69	-1.17

Table 26: Breeding Gains for Configuration 1, Calculated Using JEF-1.1 Data, and Their Deviations from the Mean Benchmark Values

Table VI	Cross-Section (barns)	Standard Deviation (%)	Deviation from the Mean Value (%)
^{238}U(n,capture)	0.307502	3.49	0.43
^{238}U(n,fission)	0.043396	5.02	5.30
^{239}Pu(n,capture)	0.594914	7.04	7.18
^{239}Pu(n,fission)	1.895509	2.10	2.20
$\alpha(^{239}\mathrm{Pu})$	0.313854	6.18	4.91
^{10}B(n,transport)	5.470800	2.18	-0.29
Fenat(n,transport)	4.842038	14.15	17.06
^{23}Na(n,transport)	4.646053	5.11	7.60
^{16}O(n,transport)	3.559627	3.04	1.59

Table 27: Central One-Group Cross-Sections for Configuration 1, Collapsed over the Central Flux Spectrum, Calculated Using JEF-1.1 Data, and Their Deviations from the Mean Benchmark Values

Table IX	Reaction Rate	Standard Deviation (%)	Deviation from the Mean Value (%)
$k_{Bsquared}$	1.149206	1.83	0.27
Fission Production			
^{239}Pu	0.418204	1.26	-0.35
^{240}Pu	0.023206	8.17	-3.51
^{241}Pu	0.091630	7.12	-2.50
^{238}U	0.089632	3.74	3.70
Total	0.632285	0.83	-0.07
Fission			
^{239}Pu	0.143388	1.34	0.39
^{238}U	0.032208	3.61	3.70
Total	0.217947	0.76	0.39
Capture			
^{239}Pu	0.045484	6.71	5.68
^{240}Pu	0.013837	19.31	6.44
^{241}Pu	0.006206	9.67	-1.65
^{238}U	0.231752	3.04	-1.86
^{16}O, ^{23}Na	0.003905	20.55	6.99
Structure	0.028704	20.14	-6.90
Total	0.332247	2.33	-0.85

Table 28: Isotopic Components of Neutron Balance Parameters for the Inner Core of Configuration 1, Calculated Using JEF-1.1 Data, and Their Deviations from the Mean Benchmark Values

Isotope(s) from JEF-1.1	Eigenvalue	% Increase Compared to (Pure) ENDF/B-VI
None	1.13438	0
All	1.11890	-1.365
^{239}Pu	1.14324	0.781
^{241}Pu	1.13499	0.053
^{238}U	1.12317	-0.988
^{23}Na	1.12678	-0.670
^{240}Pu	1.13187	-0.221
^{16}O	1.13189	-0.220
Fenat	1.13292	-0.129
^{242}Pu	1.13419	-0.017
^{235}U	1.13435	-0.003

Table 29: Eigenvalues k_∞ for the Inner Core (Configuration 1), Calculated Using ENDF/B-VI Data, and Their Percent Increase Due to the Use of JEF-1.1 Data for Individual Nuclides

Isotope and Reaction(s) from JEF-1.1	Eigenvalue	% Increase Compared to (Pure) ENDF/B-VI
None	1.13438	0
^{239}Pu	1.14324	0.781
^{239}Pu Fission and Fission Production	1.14629	1.050
^{239}Pu Fission (Nubar from ENDF/B-VI)	1.15310	1.650
^{239}Pu Nubar (Fission from ENDF/B-VI)	1.12769	-0.590
^{239}Pu Capture	1.13089	-0.308
Fission Spectrum	1.13324	-0.100
None	1.13438	0
^{238}U	1.12317	-0.988
^{238}U Inelastic Scattering	1.12107	-1.173
None	1.13438	0
^{23}Na	1.12678	-0.670
^{23}Na Inelastic Scattering	1.12799	-0.563

Table 30: Eigenvalues k_∞ for the Inner Core (Configuration 1), Calculated Using ENDF/B-VI Data, and Their Percent Increase Due to the Use of JEF-1.1 Data for Individual Reactions, for Relevant Nuclides

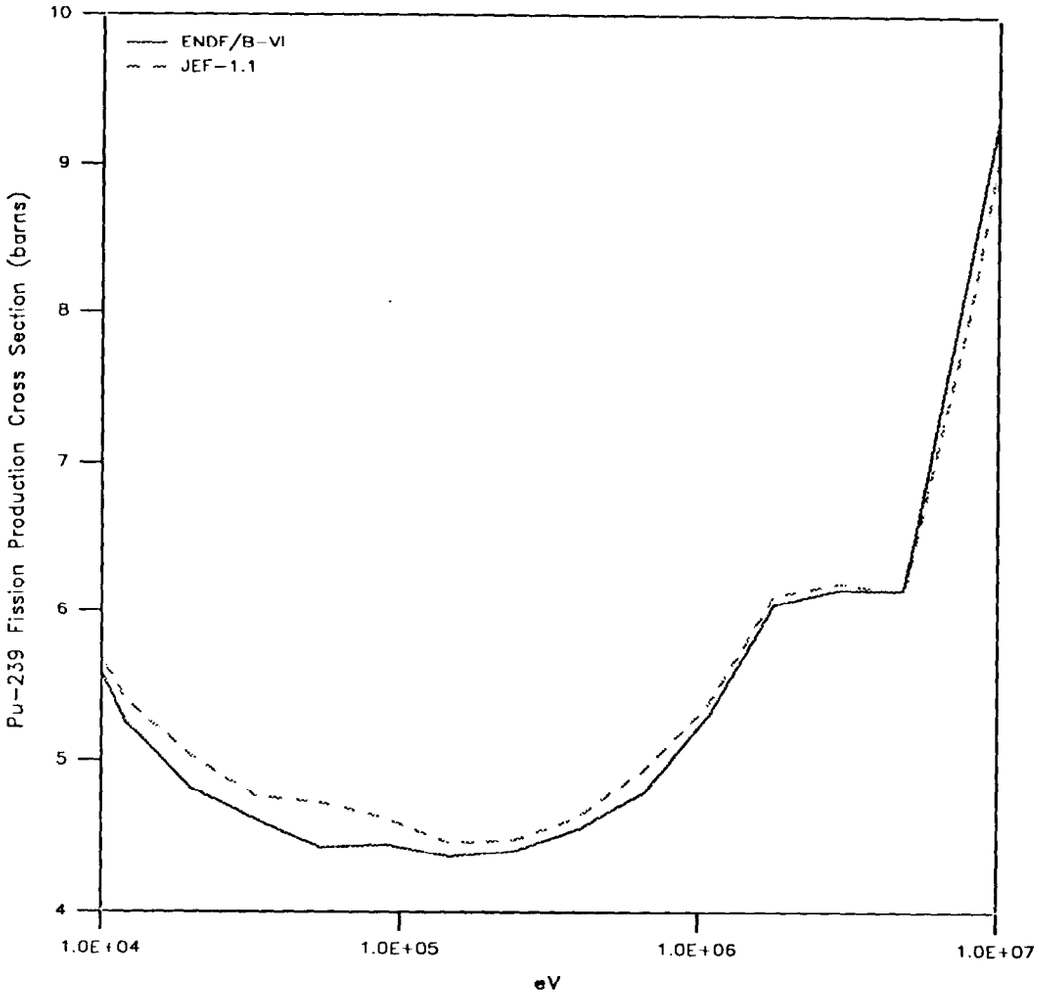

Figure 1: 33 Group Fast ^{239}Pu Fission Production Cross Section

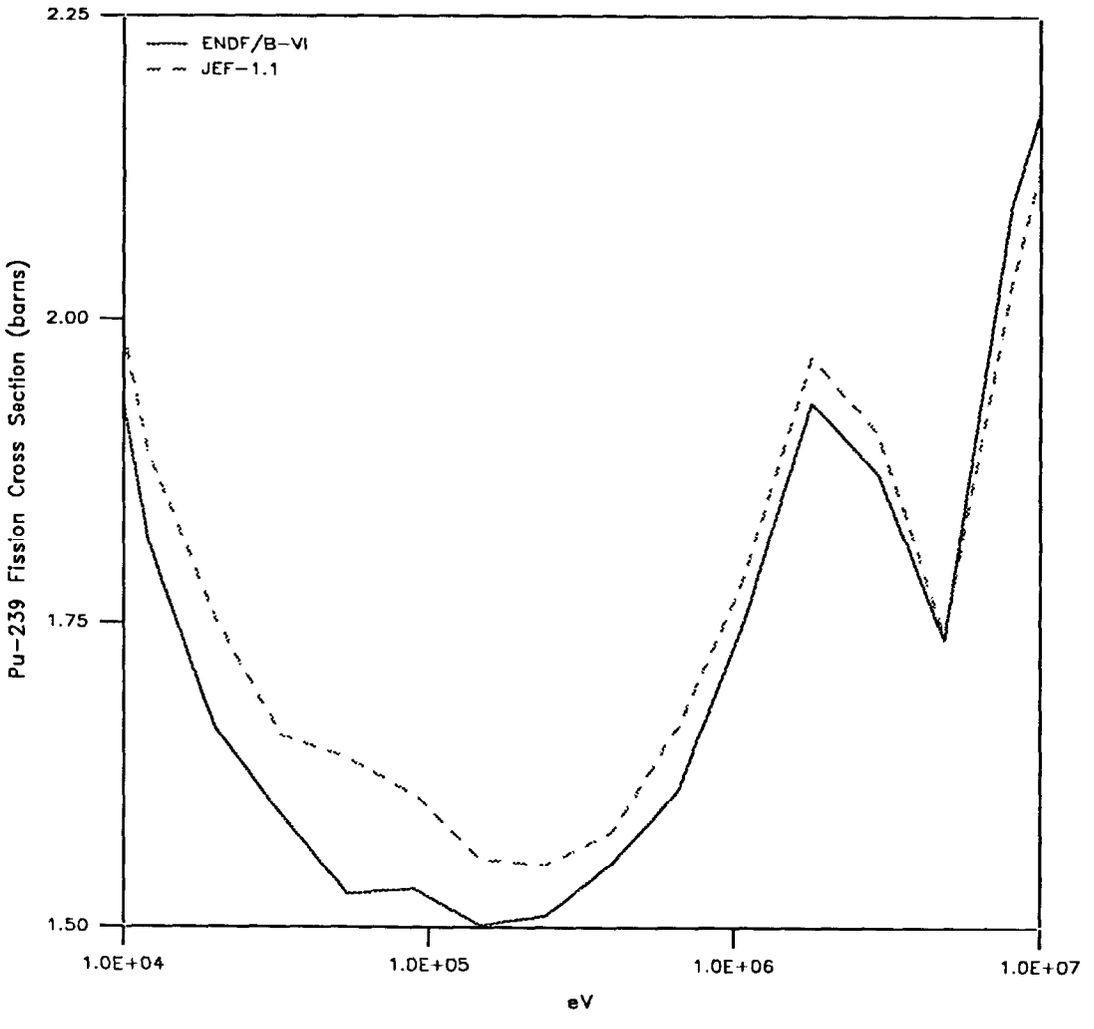

Figure 2: 33 Group Fast ^{239}Pu Fission Cross Section

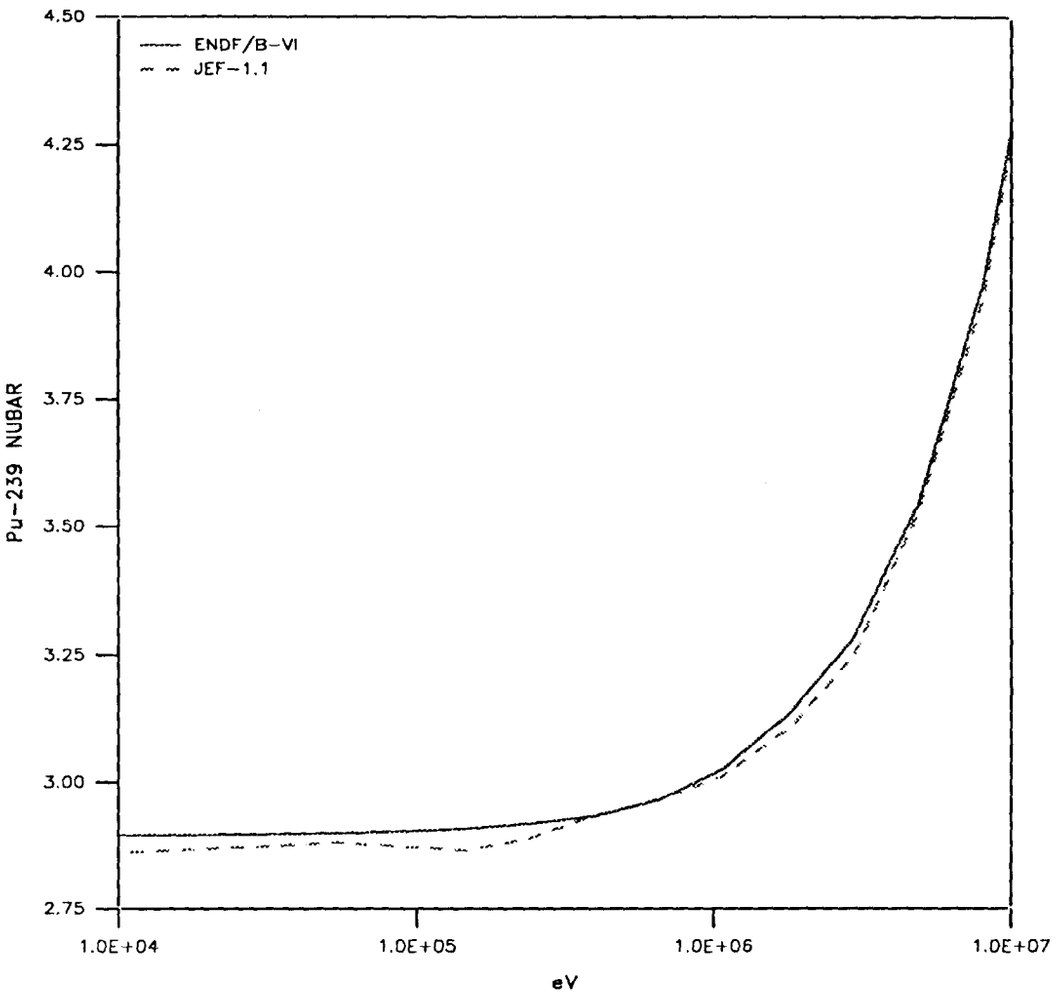

Figure 3: 33 Group Fast Nubar for ^{239}Pu

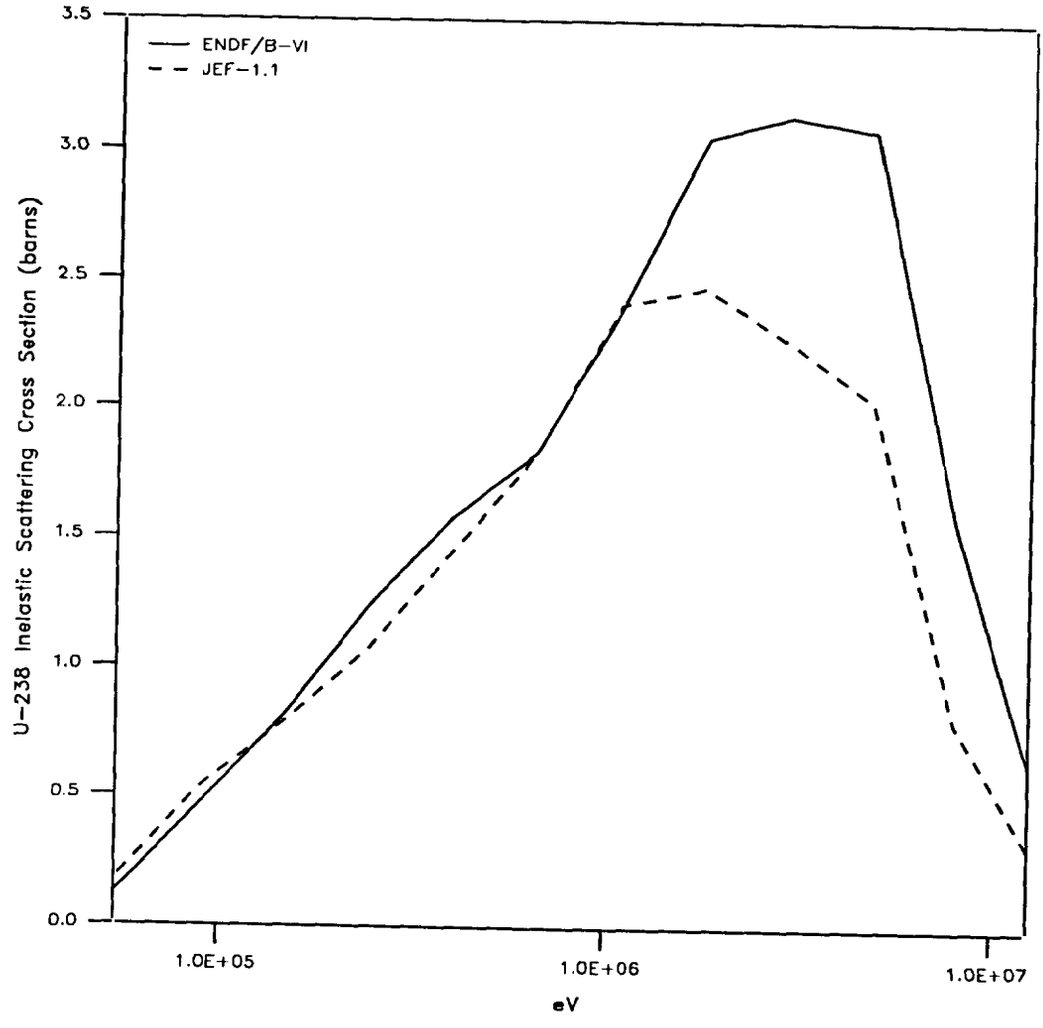

Figure 4: 33 Group Fast ^{238}U Inelastic Scattering Cross Section

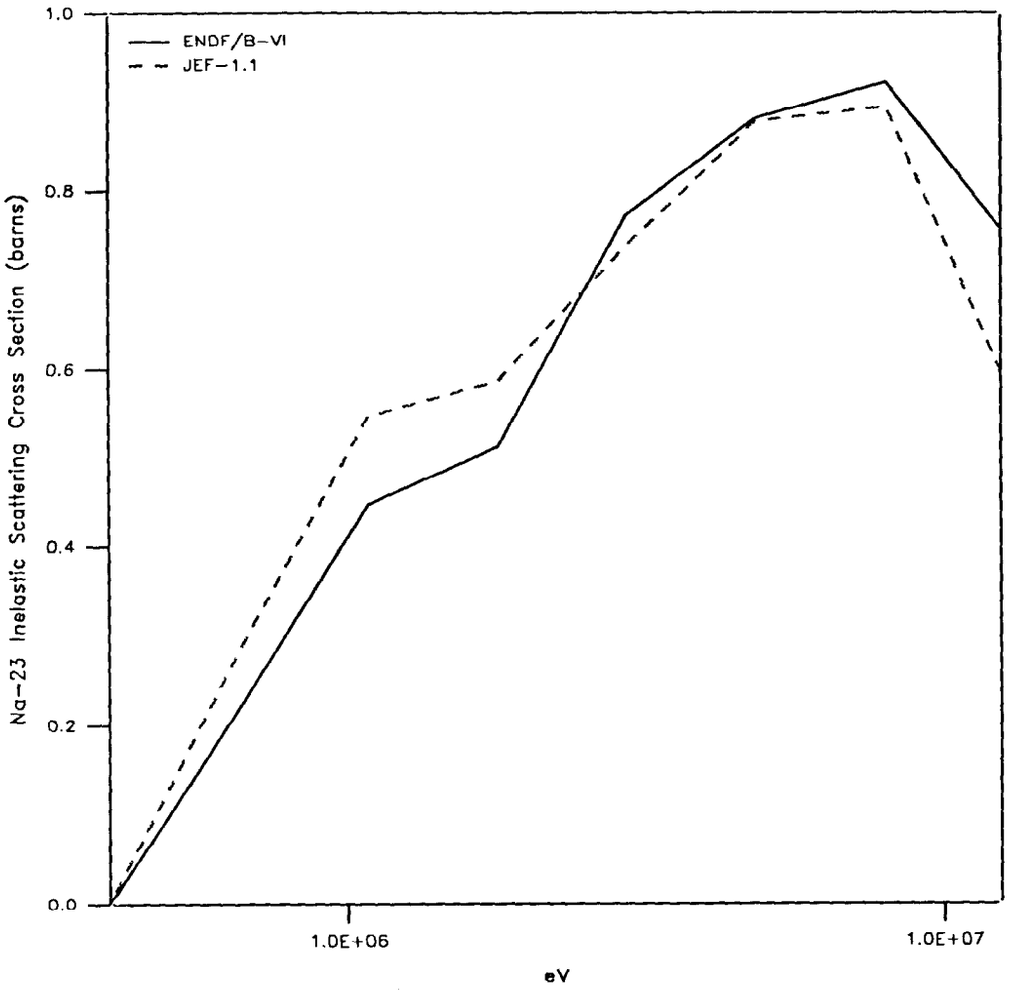

Figure 5: 33 Group Fast ^{23}Na Inelastic Scattering Cross Section

References

[1] L. G. Sage, R. D. McKnight, D. C. Wade, K. E. Freese, P. J. Collins, " Proc. of the NEACRP/IAEA Specialists Meeting on the International Comparison Calculation of a Large Sodium-Cooled Fast Breeder Reactor at Argonne National Laboratory on February 7-9, 1988, " ANL-80-78/NEA-CRP-L-243 (August 1980)

[2] H. U. Wenger, P. Wydler, " Benchmark-Rechnungen für einen schnellen Brutreaktor mit JEF-1 Neutronendaten, " Proc. Jahrestagung Kerntechnik, Kerntechnische Gesellschaft e. V., Deutsches Atomforum e. V., p. 79-82 (Mai 1989)

[3] J. Rowlands, N. Tubbs, " The Joint Evaluated File: a New Data Resource for Reactor Calculations, " Proc. of International Conference on Nuclear Data for Basic and Applied Science, Vol. 2, p. 1493, Santa Fe, New Mexico (1985)

[4] D. R. Mathews, P. Koch, " MICROX-2. An Improved Two-Region Flux Spectrum Code for the Efficient Calculation of Group Cross Sections, " Genaral Atomics Report, GA-A15009, Vol.1 (1979)

[5] C. L. Dunford, " Evaluated Nuclear Data File, ENDF/B-VI, " Proc. of International Conference on Nuclear Data for Science and Technology, Jülich, Germany (May 1991)

[6] R. W. Hardie, W. W. Little, Jr., " PERT-V: A Two-Dimensional Perturbation Code for Fast Reactor Analysis, " Battelle-Northwest, Richland, Wash. Pacific Northwest Laboratory Report, BNWL-1162 (September 1969)

[7] R. D. O'Dell, " Standard Interface Files and Procedures for Reactor Physics Codes, Version IV, " Los Alamos National Laboratory Report, LA-6941-MS (September 1977)

[8] R. E. MacFarlane, D. W. Muir, R. M. Boicourt, " The NJOY Nuclear Data Processing System, Volume I: User's Manual, " Los Alamos National Laboratory Report, LA-9303-M (ENDF-324) (1982)

[9] C. R. Eaton, J. L. Rowlands, " Processing of ENDF/B-VI Structural Material Files Using NJOY: A Problem when NAPS=1, " Private Communication, JEF-Meeting, Saclay (December 1991)

[10] S. Pelloni, " A New JEF-1 Library for Fast Breeder Calculations Processed with NJOY89.62, " Paul Scherrer Institute Internal Report, TM-41-91-13 (Sept. 1991)

[11] O. Ozer, " RESEND: A Program to Preprocess ENDF/B Materials with Resonance Files into a Pointwise Form, " Brookhaven National Laboratory Report, BNL-17134 (1972)

[12] D. E. Cullen, C. R. Weisbin, " Exact Doppler-Broadening of Tabulated Cross Sections, " Nuclear Science and Engineering, Vol. 60, page 199 (1976)

[13] R. E. Schenter, J. L. Baker, R. B. Kidman, " ETOX. A Code to Calculate Group Constants for Nuclear Reactor Calculations, " Battelle Northwest Laboratory Report, BNWL-1002 (1962)

[14] P. Wälti, P. Koch, " MICROX, A Two-Region Flux Spectrum Code for the Efficient Calculation of Group Cross Sections, " Gulf General Atomic Report, Gulf-GA-A10827 (1972)

[15] R. E. MacFarlane, D. W. Muir, " The NJOY Nuclear Data Processing System, Volume III: The GROUPR, GAMINR, and MODER Modules, " Los Alamos National Laboratory Report, LA-9303-M (ENDF-324) (July 1986)

[16] D. R. Mathews, Private Communication, Paul Scherrer Institute (March 26, 1990)

[17] D. R. Mathews, J. Stepanek, S. Pelloni, C. E. Higgs, " The NJOY Nuclear Data Processing System: the MICROR Module, " Paul Scherrer Institute Report, EIR Report 539 (December 1984)

[18] S. Pelloni, P. Grimm, D. R. Mathews, J. M. Paratte, " Validation of Light Water Reactor Calculation Methods and JEF-1-Based Data Libraries by TRX and BAPL Critical Experiments, " Nuclear Technology, Vol. 94, p. 15-27 (April 1991)

[19] R. E. MacFarlane, " TRANSX-CTR: A Code for Interfacing MATXS Cross Section Libraries to Nuclear Transport Codes for Fusion System Analysis, " Los Alamos National Laboratory Report, LA-9863-MS (February 1984)

[20] M. Caro, Private Communication, Paul Scherrer Institute (1991)

[21] R. D. O'Dell, F. W. Brinkley, D. R. Marr, " User's Manual for ONEDANT: A Code Package for One-Dimensional Diffusion Accelerated Neutral Particle Transport, " Los Alamos National Laboratory Report, LA-7396-M (September 1986)

[22] D. C. George, R. J. LaBauve, Private Communication (1991)

[23] D. R. Mathews, " The PSI Version of the PERT-V Code, " Paul Scherrer Institute Internal Report, TM-41-91-29 (September 1991)

[24] D. R. Mathews, Private Communication, Paul Scherrer Institute (January 1992)